JARQ 48 (4), 465 - 470 (2014) http://www.jircas.affrc.go.jp

Application of Multi-temporal TerraSAR-X Data to Map Winter Wheat Planted Areas in Hokkaido, Japan

Rei SONOBE[1]*, Hiroshi TANI[2], Xiufeng WANG[2], Nobuyuki KOBAYASHI[3], Atsushi KIMURA[4] and Hideki SHIMAMURA[4]

[1] Graduate School of Agriculture, Hokkaido University (Sapporo, Hokkaido 060-8589, Japan)
[2] Research Faculty of Agriculture, Hokkaido University (Sapporo, Hokkaido 060-8589, Japan)
[3] Hokkaido Intellect Tank (Sapporo, Hokkaido 060-0004, Japan)
[4] PASCO Corporation (Meguro, Tokyo 153-0043, Japan)

Abstract

Winter wheat is an important crop for many countries, and monitoring of its planted area is considered important. Optical sensors have been used to monitor agricultural land, and have shown good classification and monitoring capabilities. However, observations using optical sensors sometimes suffer from interference due to cloud cover or rain. In contrast, synthetic aperture radars (SAR) can be used for Earth observation even under rainy, cloudy or dark conditions, hence SAR is expected to be effective in monitoring agricultural fields and identifying winter wheat fields. The objective of this study is to analyze the potential of TerraSAR-X dual images, in the StripMap mode, for mapping winter wheat planted areas. Using the separability statistic (*D*), it emerged that the sigma naught acquired in mid-July possesses great potential. The method applied in this study has an overall accuracy exceeding 96% for HH and VV polarization data for identifying winter wheat fields.

Discipline: Information technology
Additional key words: backscattering coefficient, satellite, crop types identification

Introduction

Remote sensing techniques have been used in agricultural fields to classify vegetation and estimate soil moisture and physiological parameters and are primarily based on the use of multispectral data. However, observations using optical sensors sometimes suffer from interference due to cloud cover or rain. In contrast, synthetic aperture radars (SAR) can be used for Earth observation even under rainy, cloudy or dark conditions.

In microwave remote sensing, the backscattering coefficients of L-band and sometimes C-band are related not only to vegetation but also soil moisture and surface roughness in most agricultural fields (Sonobe & Tani 2009). The effect of vegetation canopy is the main factor impacting on X-band data over vegetated fields. The intensity of incident energy scattered by vegetation is primarily a function of the canopy architecture, such as the size, shape and orientation of canopy components (leaves, stalks, and fruit), the dielectric properties of the crop canopy and the cropping characteristics (plant density and row direction) (McNairn et al. 2009). Over the last few decades, radar remote sensing data have also been increasingly utilized for vegetation characterization and crop monitoring as well as yield prediction. Recently, TerraSAR-X was launched on June 15, 2007 and X-band SAR data were made widely available. The objective of the mission was to develop an operational spaceborne X-band synthetic aperture radar (SAR) system to produce various products for commercial and scientific use. TerraSAR-X delivers X-band SAR data at a high spatial resolution of 2.5 to 6 m within a 30-km swathe in Stripmap mode. Furthermore, several studies have proven its high geometric accuracy[1]. Although the operational lifetime is 5 years, TanDEM-X, with the same specifications, was launched on June 21, 2010, and the launch of SEOSAR/PAZ is planned in 2014, hence, regular observations will be possible in future.

Studies on rice monitoring and mapping using SAR data have increased, some of which have used multi-temporal RADARSAT C-band data in HH polarization and revealed high correlations between backscattering coefficients and plant height and age (Chakraborty et al. 2005, Shao et al. 2001). These examples have been used in agricultural man-

*Corresponding author: reysnb@env.agr.hokudai.ac.jp
Received 11 July 2013; accepted 14 February 2014.

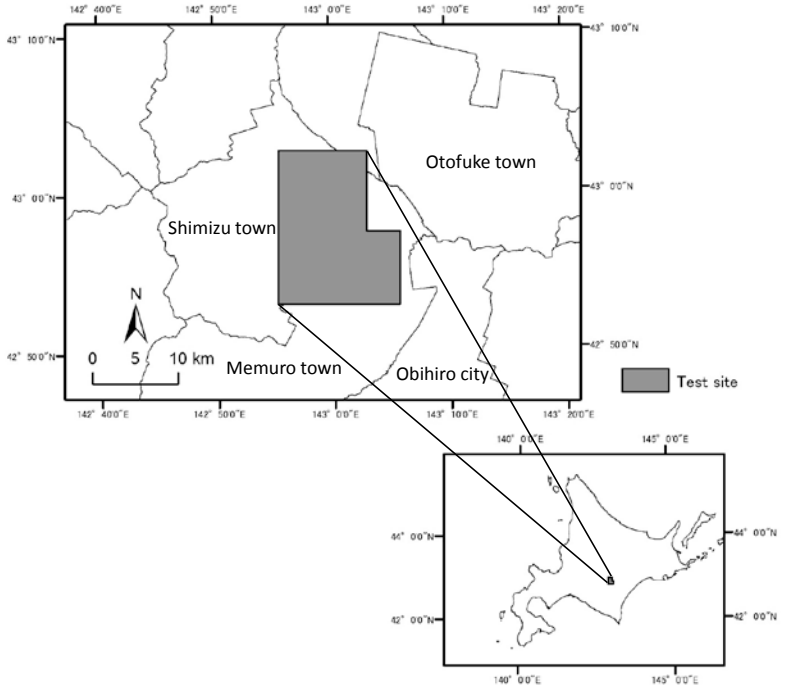

Fig. 1. Test site located southeast of Hokkaido, Japan

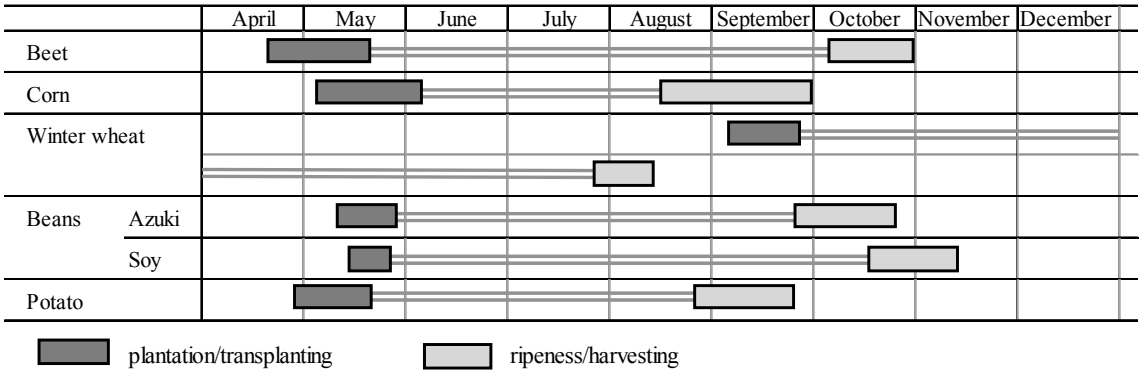

Fig. 2. Cultivation calendar for the crops in this study area

agement to identify rice paddy fields. Compared with other crops, winter wheat has a unique scattering pattern due to seeding in the fall. However, the potential use of satellite-based SAR data for mapping winter wheat fields is not fully understood (Gebhardt et al. 2012). The objectives of this study are to analyze the separability of winter wheat from other crops using TerraSAR-X data and then map the winter wheat planted areas.

Materials and methods

The experimental area of this study is the farming area covering an area of approximately 20.5 km² in the western Tokachi plains, Hokkaido, Japan (Fig. 1). The dominant crops of winter wheat, pulses (azuki and soy), potato, beet and corn (dent corn and sweetcorn) are cultivated on 4,627 fields in the study area. The cultivation calendar for the crops in this study area is presented in Figure 2.

TerraSAR-X data were acquired between May 2 and November 5, 2009. Details of the acquired data are presented in Table 1. TerraSAR-X is a side-looking X-band synthetic aperture radar (SAR) based on active phased array antenna technology (Roth et al. 2004) and flies in a sun-synchronous dawn-dusk 11 day repeat orbit at an altitude of 514 km at the equator.

In this study, L1B Enhanced Ellipsoid Corrected

Table 1. Characteristics of the satellite data

Date	Sensor/Mode	Incidence angle (°)	Pixel spacing (m)	Orbit	Polarization
May 2, 2009 May 13, 2009 May 24, 2009 June 4, 2009 June 26, 2009 July 7, 2009 July 18, 2009 July 29, 2009 August 9, 2009 August 31, 2009 September 11, 2009 September 22, 2009 October 3, 2009 October 14, 2009 October 25, 2009 November 5, 2009	TerraSAR-X/ StripMap	42.3	2.75	Ascending	HH, VV

(EEC) products operated in Stripmap mode were used. The TerraSAR-X images were converted from digital numbers to sigma naught using the following equation (Infoterra GmbH 2008):

$$\sigma^0 = 20\log_{10} DN + 10\log_{10} CF + 10\log_{10}(\sin\theta_{loc}) , \quad (1)$$

where σ^o is sigma naught in dB, DN is a TerraSAR-X image digital number, CF is the calibration and processor scaling factor, and θ_{loc} is the local incidence angle (Ager & Bresnahan 2009). To compensate for spatial variability and avoid problems related to uncertainty in georeferencing, the average σ^o (dB) was assigned to each field.

Sigma naught values were calculated for 4,627 fields (533 azuki fields, 722 beet fields, 625 corn fields, 947 potato fields, 301 soy fields and 1,499 winter wheat fields) in the study area. The reference data were provided by Tokachi Nosai as a polygon-shaped file, in which the position of the fields and attribute data such as crop type were included.

The separability statistic (D) is used to evaluate separability (Miettinen & Liew 2011). The D was calculated to compare the statistical separability of winter wheat using sigma naught as follows (Kaufman & Remer 1994):

$$D = \frac{\left|\bar{x}_1 - \bar{x}_2\right|}{s_1 + s_2} , \quad (2)$$

where $\bar{x}_i$ and s_i are the mean and standard deviation of the sigma naught values of analyzed crop types, respectively, and defined as follows:

$$\bar{x}_i = \frac{\sum_{k=1}^{n} x_{i,k}}{n} , \quad (3)$$

$$s_i = \sqrt{\frac{\sum_{k=1}^{n} (x_{i,k} - \bar{x}_i)^2}{n}} , \quad (4)$$

where $x_{i,k}$ is a pixel value, which is equal to a sigma naught value in dB units, k is a given pixel, and n is the number of pixels of a given crop type (i). The D normalizes the difference in the means by the sum of standard deviations. The standard theory on feature separation is that features are well separated if the distance between the class mean values is large compared with the standard deviation (Shi et al. 1994). In the case of D = 1, this allows an overlap of nearly 16% of the samples. We visually verified that the histograms of the data acquired on July 18 revealed high D values.

Finally, the thresholds were calculated using Otsu's method (Otsu 1979) to distinguish between winter wheat and other crops and the accuracy of the results was assessed by comparison with the reference data provided by Tokachi Nosai. In addition to the overall accuracy, the accuracies of the user and producer were also calculated.

Results and discussion

Table 2 presents the D values between winter wheat and the other five crop types for all obtained TerraSAR-X data. On May 2, the values were very low because the winter wheat fields were sparsely vegetated and the other fields had just been seeded and their soil was nearly bare. However, the difference in growth became clear over time. The main backscatter response was volume scattering in the winter wheat fields, whereas that of other crops was surface scattering. Consequently, low backscattering for winter wheat was observed and the D values increased until the period from June 26 to July 18. Afterward, the winter wheat plants became mature, whereupon diffuse reflection was the predominant response in the winter wheat fields, and the sigma naught values were high, which meant the difference in backscattering between the winter wheat fields and others became unclear and the D values declined. The winter wheat and other crops were harvested in mid-August.

The D values obtained here indicate that the sigma naught values acquired during the period June 26 to July 18

Table 2. Separability of wheat from the other five crop species in TerraSAR-X data. The underlined characters show that these values are optimal for each species

	Target for comparison	Separability statistic D							
		May 2	May 13	May 24	June 4	June 26	July 7	July 18	July 29
HH	Azuki	0.219	0.487	0.485	0.093	0.333	0.554	0.853	0.471
	Beet	0.275	0.295	0.014	0.694	1.220	1.272	1.139	0.681
	Corn	0.230	0.189	0.346	0.174	0.527	0.685	0.902	0.557
	Poteto	0.207	0.198	0.026	0.734	1.088	1.012	0.729	0.500
	Soy	0.223	0.400	0.471	0.196	0.551	0.665	0.856	0.522
VV	Azuki	0.056	0.622	0.362	0.350	0.615	0.692	0.849	0.678
	Beet	0.140	0.463	0.081	0.763	1.421	1.372	1.090	0.847
	Corn	0.069	0.438	0.197	0.377	0.693	0.700	0.761	0.636
	Poteto	0.070	0.371	0.086	0.827	1.359	1.211	0.792	0.745
	Soy	0.058	0.555	0.344	0.413	0.789	0.769	0.798	0.681

	Target for comparison	Separability statistic D							
		August 9	August 31	September 11	September 22	October 3	October 14	October 25	November 5
HH	Azuki	0.227	0.182	0.322	0.422	0.330	0.150	0.023	0.073
	Beet	0.536	0.558	0.610	0.698	0.720	0.542	0.476	0.211
	Corn	0.367	0.255	0.291	0.205	0.061	0.005	0.018	0.034
	Poteto	0.389	0.397	0.297	0.194	0.021	0.021	0.009	0.055
	Soy	0.232	0.120	0.270	0.285	0.249	0.215	0.107	0.015
VV	Azuki	0.405	0.333	0.375	0.452	0.325	0.159	0.015	0.114
	Beet	0.658	0.627	0.657	0.748	0.747	0.581	0.508	0.239
	Corn	0.396	0.251	0.271	0.216	0.083	0.019	0.021	0.037
	Poteto	0.524	0.422	0.287	0.203	0.020	0.014	0.035	0.059
	Soy	0.418	0.254	0.333	0.331	0.218	0.175	0.099	0.014

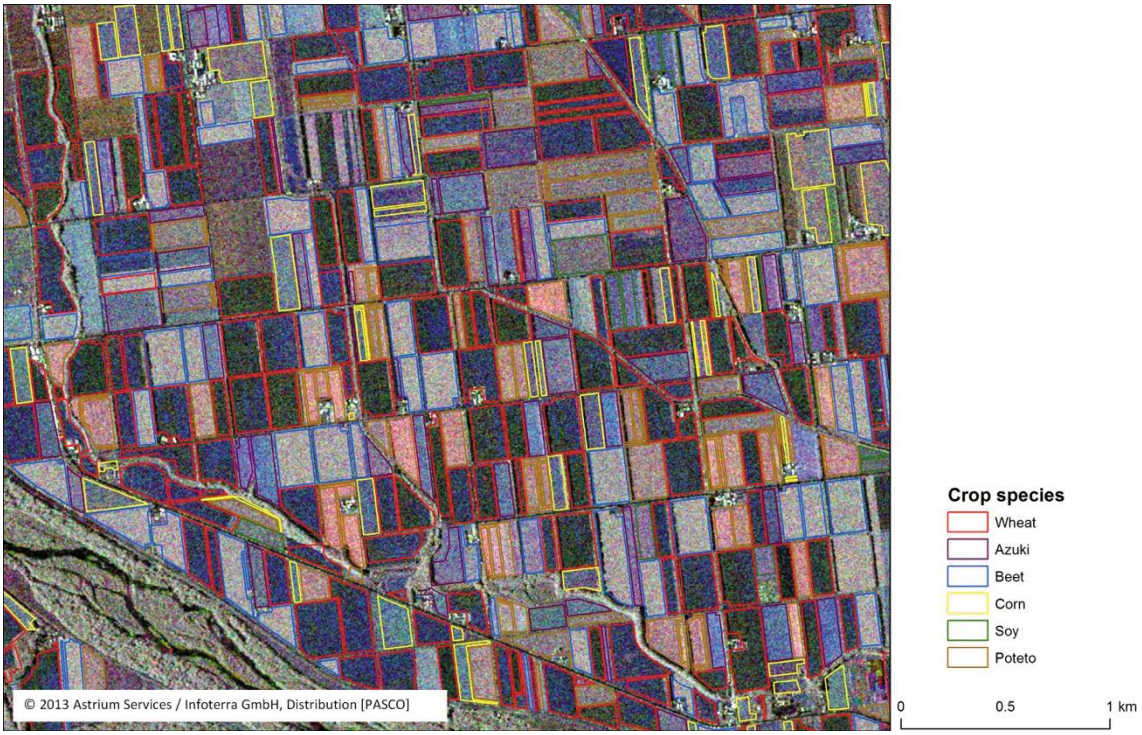

Fig. 3. Color composite image illustrating different types of backscattering (RGB: VV on June 26, HH on July 7, VV on July 18)

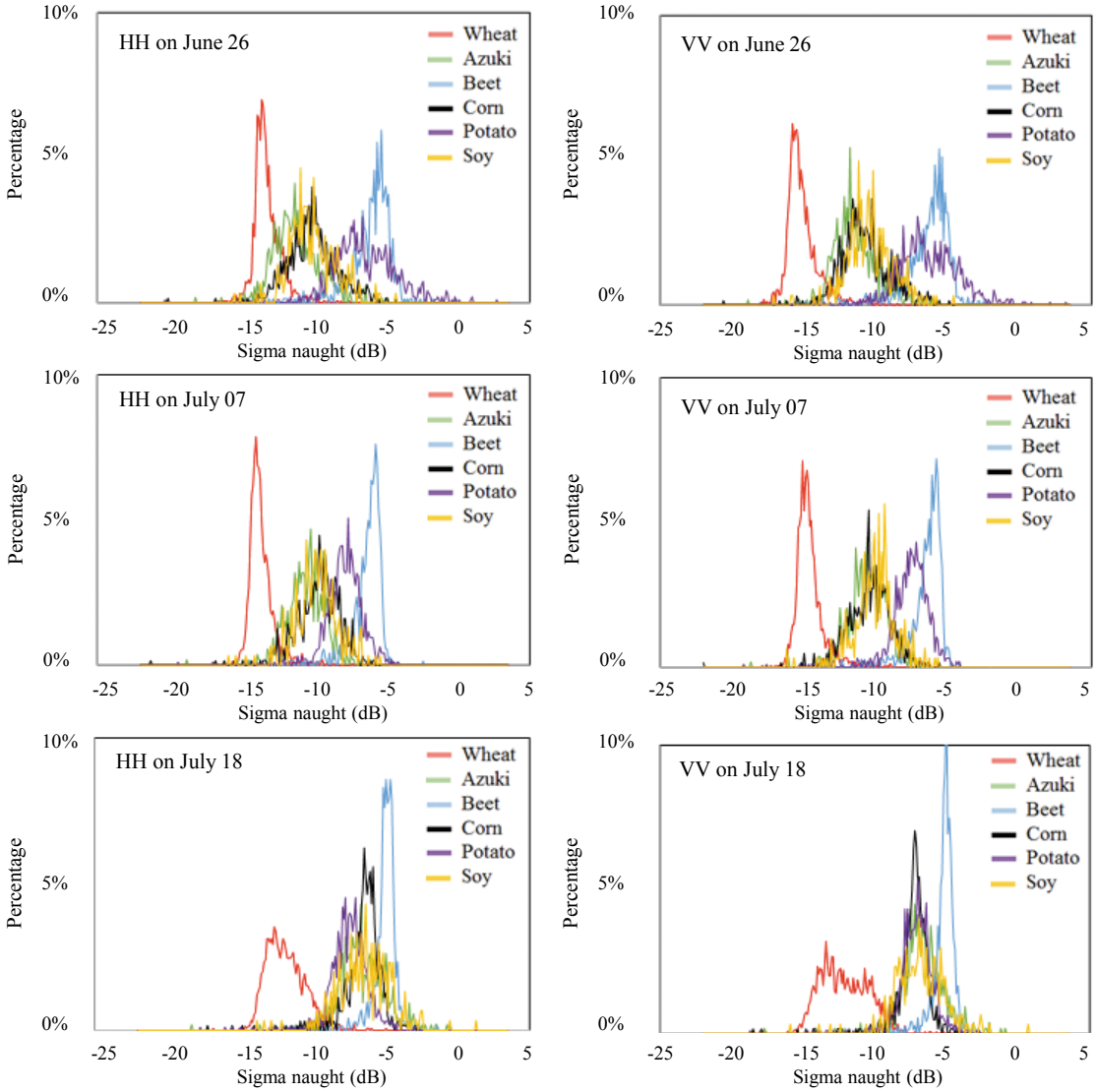

Fig. 4. Histograms of crop types in sigma naught (dB)

Table 3. Accuracy assessment for HH polarization data

Result of discriminant	Reference data		User's accuracy
	Wheat	Others	
Wheat	1,456	118	92.5%
Others	43	3,010	98.6%
Producer's accuracy	97.1%	96.2%	

Overall accuracy: 96.5%

Table 4. Accuracy assessment for VV polarization data

Result of discriminant	Reference data		User's accuracy
	Wheat	Others	
Wheat	1,449	119	92.4%
Others	50	3,009	98.4%
Producer's accuracy	96.7%	96.2%	

Overall accuracy: 96.3%

are useful to identify winter wheat fields. Figure 3 shows the color composite image using the period (VV on June 26 for red, HH on July 7 for green and VV on July 18 for blue). In this image, the winter wheat fields are definitively identified because of the low backscattering by diffuse reflection.

Figure 4 presents histograms of the sigma naught values of HH and VV polarization during the period June 26 to July 18. Overlaps are observed between winter wheat fields and other crops on June 26 and July 7; the winter wheat field data on July 18 are clearly separated from the others. It was caused by the increase in sigma naught values with growth for soy, azuki and corn, which implies that the separation of the winter wheat fields using a certain threshold value is possible. We employed Otsu's method to determine the threshold values and those obtained by the method were -9.1 and -9.0 dB for HH and VV polarizations, respectively.

The accuracy of the identification was confirmed using the reference data as presented above. The results of the accuracy assessments are summarized in Tables 3 and 4. The method was found to yield overall accuracies of 96.5 and 96.3% for HH and VV polarizations, respectively.

Conclusions

In this study, TerraSAR-X HH and VV polarization data operated in Stripmap mode were used and the potential of X-band SAR on-board satellite data for mapping winter wheat planted areas was analyzed.

Sigma naught values were collected from 4,627 fields (533 azuki fields, 722 beet fields, 625 corn fields, 947 potato fields, 301 soy fields and 1,499 winter wheat fields), and the separability statistic (D) was calculated. These D values indicate that the sigma naught values acquired during the period June 26 to July 18 are useful to identify winter wheat fields. Furthermore, using histograms, it emerged that the winter wheat field data on July 18 were separated from the other crops using a simple method.

To determine the threshold values, Otsu's method was applied and the identification of winter wheat fields using the threshold values was possible with overall accuracy exceeding 96% for HH and VV polarization data.

Acknowledgements

For the in-situ survey and analysis, we received great assistance from Mr. Yasuhito Kojima, Ms. Shiming Jiang and Mr. Toshinori Soma of Hokkaido University. The authors are thankful to Tokachi Nosai for providing the field data.

References

Ager, T. P. & Bresnahan, P. C. (2009) Geometric precision in space radar imaging: results from TerraSAR-X. Proc. ASPRS 2009 Annu. Conf., 9-13.

Chakraborty, M. et al. (2005) Rice crop parameter retrieval using multi-temporal, multi-incidence angle Radarsat SAR data. *ISPRS J. Photogramm. Remote Sens.*, **59**, 310-322.

Gebhardt, S. et al. (2012) A comparison of TerraSAR-X Quad-pol backscattering with RapidEye multispectral vegetation indices over rice fields in the Mekong Delta, Vietnam. *Int. J. Remote Sens.*, **33**, 7644-7661.

Infoterra GmbH: Radiometric calibration of TerraSAR-X data: http://www2.astrium-geo.com/files/pmedia/public/r465_9_tsxx-itd-tn-0049-radiometric_calculations_i1.00.pdf.

Kaufman, Y. J. & Remer, L. A. (1994) Detection of forests using mid-IR reflectance: an application for aerosol studies. I*EEE Trans. Geosci. Remote Sens.*, **32**, 672-683.

McNairn, H. et al. (2009) Integration of optical and Synthetic Aperture Radar (SAR) imagery for delivering operational annual crop inventories. *ISPRS J. Photogramm. Remote Sens.*, **64**, 434-449.

Miettinen, J. & Liew, S. C (2011) Separability of insular Southeast Asian woody plantation species in the 50 m resolution ALOS PALSAR mosaic product. *Remote Sens. Lett.*, **2**, 299-307.

Otsu, N. (1979) A Threshold Selection Method from Gray-Level Histograms. *IEEE Trans. Syst. Man Cybern.*, **9**, 62-66, 1979.

Roth, R. et al. (2004) Geocoding of TerraSAR-X data, Proc. Int. 20th ISPRS Congr., 840-844.

Shao, Y. et al. (2001) Rice monitoring and production estimation using multitemporal RADARSAT. *Remote Sens. Environ.*, **76**, 310-325.

Shi, J. et al. (1994) Snow mapping in Alpine regions with Synthetic Aperture Radar. *IEEE Trans. Geosci. Remote Sens.*, **32**, 152-158.

Sonobe, R. & Tani, H (2009) Application of the Sahebi model using ALOS/PALSAR and 66.3 cm long surface profile data. *Int. J. Remote Sens.*, **30**, 6069-6074.